

10-22-81
24
NTS

U

37852

SAND81-1253
Unlimited Distribution

MASTER

NTS-1290

PRELIMINARY TRANSPORT ANALYSES FOR
DESIGN OF THE TUFF RADIONUCLIDE-
MIGRATION FIELD EXPERIMENT

K. L. Erickson and D. R. Fortney



Sandia National Laboratory

HYDROLOGY DOCUMENT NUMBER 183

THIS DOCUMENT HAS BEEN REPRODUCED
FROM NRC MICROFICHE HOLDINGS BY
THE DOCUMENT MANAGEMENT BRANCH,
DIVISION OF TECHNICAL INFORMATION
AND DOCUMENT CONTROL

FOR INFORMATION ABOUT MICROGRAPHIC SERVICES
INCLUDING EQUIPMENT CALL: 28137

FOR DETAILS ON:

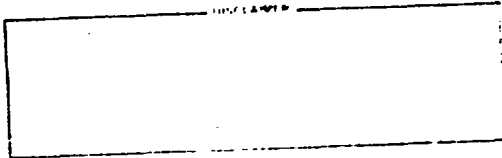
MICROFICHE BLOWBACK SERVICES CALL: 28076

APERTURE CARD BLOWBACK SERVICES CALL: 28076

MICROFICHE OR APERTURE CARD DUPLICATION CALL: 28076

FOR EQUIPMENT REPAIRS CALL: 28397

**PORCTIONS
OF THIS
DOCUMENT
ARE
ILLEGIBLE**



SAND81-1253
UNLIMITED DISTRIBUTION

Preliminary Transport Analyses for Design
of the Tuff Radionuclide-Migration Field Experiment

K. L. Erickson
and
D. P. Fontney

Sandia National Laboratories
Albuquerque, New Mexico 87185

ABSTRACT

As part of the Nevada Nuclear Waste Storage Initiative project, Los Alamos, Sandia and Argonne National Laboratories will cooperatively conduct several small-scale field experiments to evaluate the potential for radionuclide transport resulting from fluid flow through joints or fractured porous rocks. Preliminary radionuclide transport analyses have been conducted in order to obtain guidance for experimental design, operating conditions for such field experiments, selection of experimental sites, and designing experimental equipment commensurate with those operating conditions. The transport analyses were based on available experimental data and were conducted to examine the general behavior of a hypothetical experiment involving an idealized joint, which could be either a natural or man-made fracture, a fault, or a joint in plate. In the idealized joint, modeled as two semi-infinite, parallel plates confining an aqueous solution, the flow, transport of dissolved species, and the rate of sorption are considered to be dominated by groundwater flow through the joint by diffusion into and simultaneous sorption into the porous rock plates bounding the joint.

The equations for radionuclide transport in the joint are derived from a matrix derivation of the general diffusion equation. The development of the equations is based on the following conditions for a hypothetical field experiment: (1) the joint is a natural or man-made fracture, a fault, or a joint in plate; (2) the joint is modeled as two semi-infinite, parallel plates confining an aqueous solution; (3) the flow, transport of dissolved species, and the rate of sorption are considered to be dominated by groundwater flow through the joint by diffusion into and simultaneous sorption into the porous rock plates bounding the joint.

calculated for the hypothetical case; however, the general trends in behavior as a function of operating conditions should be similar. Some implications which the analyses of the hypothetical experiment have for an actual field experiment appear to be as follows: (1) fluid velocities much greater than the natural fluid velocities will be required to conduct meaningful experiments; (2) well defined concentration profiles in the bulk rock bounding the joint should provide the primary data for validation of radionuclide transport models; and (3) the development of the desired profiles in the bulk rock will be much more sensitive to fluid velocity and plate spacing than to sorption distribution coefficient.

TABLE OF CONTENTS

	Page No.
ABSTRACT	1
INTRODUCTION	1
EXPERIMENTAL BASIS	1
IDEALIZED JOINT	1
Definition	1
Mathematical Description	11
DESIGN ANALYSES	11
Hypothetical Experiment	11
Application to Design Analysis	17
Factors	17
Performance Curves	17
Step Input	21
Square-Wave Input	27
Activity Profiles in the Bulk Rock	29
Square-Wave Input	29
DISCUSSION	41
Principal Results for the Hypothetical Experiment	41
Lessons for an Actual Experiment	44
CONCLUSIONS AND RECOMMENDATIONS	47
REFERENCES	48
APPENDIX	49

operating conditions. The transport analyses were based on available experimental data regarding dominant chemical phenomena and were conducted to examine the general behavior of a hypothetical experiment involving an idealized joint, which could represent a natural or man-made fracture, a fault, or a parting plane. In the text below the experimental basis for selecting the idealized joint is briefly summarized, and the idealized joint is defined. Radionuclide transport in the idealized joint is then mathematically described for specified physical and chemical parameters and the resulting models are applied to the design of a hypothetical field experiment involving the idealized joint. Criteria for determining optimal operating conditions are developed, and the effects which perturbations in various parameter values would have on experimental results are evaluated. Finally, the principal results of the analyses for the hypothetical experiment are summarized, and the implications which those results have for the design of actual field experiments are discussed.

EXPERIMENTAL BASIS

The equilibria and rates for sorption of radionuclides by samples of nonwelded tuff such as that occurring in G-Tunnel at the Nevada Test Site are being experimentally investigated (1). The radionuclides used in these investigations include ^{22}Na , ^{137}Cs , ^{90}Sr , and ^{152}Eu . For nuclides such as ^{22}Na , ^{137}Cs , and ^{90}Sr which generally behave as simple ions in aqueous solutions, the available data indicate that the rate at which samples of

nonwelded tuff remove dissolved radionuclides from well mixed solutions is apparently dominated by molecular diffusion through the pore water in the bulk rock and by simultaneous sorption of the radionuclides by the solid phases. In this regard, it appears that the bulk rock, consisting of both pore water and solid phases, can be considered as a quasi-homogeneous medium for which the assumption of local sorption equilibrium between pore water and solid phases is a reasonable first approximation. It further appears that the safe procedure would be to use the rates at which dissolved radionuclides are removed from aqueous solutions flowing through sufficiently porous media. For well-scale field experiments where the flow rates and conditions are similar to those discussed above, the results of the experiments should be sufficiently accurate to provide a reasonable basis for the point can be considered very well in extent.

APPENDIX I

In the experimental results summarized above, the flow rate was defined as Q and the cross-sectional area of the porous medium was defined as A . The flow rate Q is defined as the volume of fluid that flows through a cross-sectional area A in a given time interval t . The cross-sectional area A is defined as the area of the porous medium perpendicular to the direction of flow. The flow rate Q is defined as the volume of fluid that flows through a cross-sectional area A in a given time interval t . The cross-sectional area A is defined as the area of the porous medium perpendicular to the direction of flow.

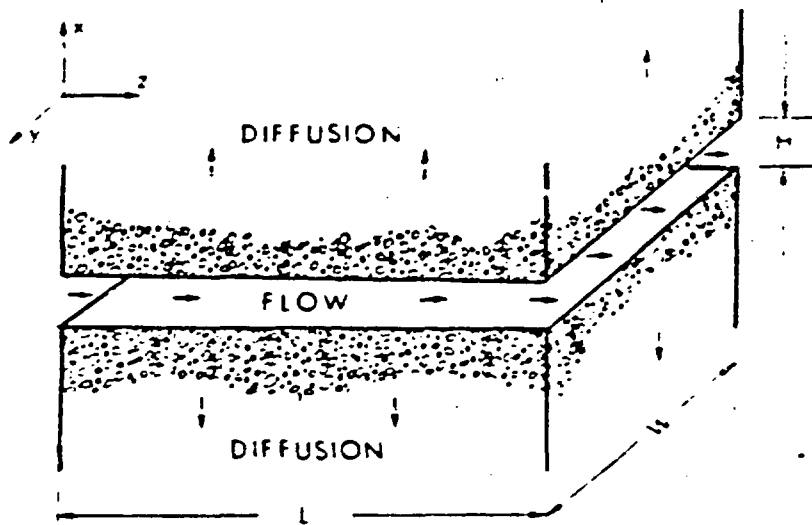


Fig. 1. Schematic representation of a linear reactor having uniform rectangular cross-section.

... fluid motion is laminar, and
... independent of the
... in all directions in the
... :

... diffusion through the
... equilibrium exists between
... phases:

... phase (fluid) ...
... are present only at
... ions or low molecular
... , ... , ...

... between the parallel plates
... with δ , ...

... the ...
... , ...

...
... , ...

...
... , ...

...
... , ...

effects due to nuclear decay and competing chemical reactions are negligible.

Mathematical Description

The above definition implies that the physical and chemical parameters of the system shown in Fig. 1 are such that it is assumed that:

1. in the flowing fluid the radionuclide flux due to advection in the z-direction is much greater than the flux due to diffusion in that direction;
2. the concentration gradient in the x-direction in the flowing fluid is negligible;
3. in the rock the radionuclide flux due to advection in the x-direction is large relative to the flux in the z-direction;
4. radionuclide concentrations are sufficiently dilute so that Fick's law, with constant diffusion coefficient, is a reasonable approximation, and the parabolic velocity profile can be approximated by a uniform average velocity v .

The partial differential equations describing mass transfer in the flowing fluid in the standing rock shown in Fig. 1 are as follows: the material balance for the flowing fluid is

$$\frac{\partial C}{\partial t} + v \frac{\partial C}{\partial z} = D \frac{\partial^2 C}{\partial x^2} \quad (1)$$

where C is the radionuclide concentration in the flowing fluid.

f

... the ... of the ...
... the ... of the ...
... the ... of the ...
... the ... of the ...

... the ... of the ...
... the ... of the ...
... the ... of the ...
... the ... of the ...

$$\frac{\partial \psi}{\partial z} = F(z, t)$$

where $F = 0$ and $\psi = 0$ at the interface between the fluid and the wall. The following initial conditions are assumed:

$$\begin{aligned} \psi(x, y, z, 0) &= 0 \text{ for all } z \\ \frac{\partial \psi}{\partial x}(x, y, z, 0) &= 0 \text{ for all } x, y, \text{ and } z \end{aligned}$$

The function $F(t)$ is a step input

$$F(t) = \begin{cases} 0 & \text{for } t < 0 \\ F_0 & \text{(constant) for } t > 0 \end{cases}$$

The solutions to Eqs. 1-3 are as follows:

$$\psi(x, y, z, t) = \dots$$

$$\frac{\partial \psi}{\partial x} = \dots$$

$$\frac{\partial \psi}{\partial y} = \dots$$

$$\frac{\partial \psi}{\partial z} = \dots$$

$$\frac{\partial \psi}{\partial t} = \dots$$

$$\psi = \dots$$

$$\dots$$

... input.

$$\begin{cases}
 0 & \text{for } t < 0 \\
 a & \text{for } 0 \leq t < b \\
 0 & \text{for } t \geq b
 \end{cases}$$

... the solutions to Eqs. 1, 2, and 3 are ...
 ... 4, 5, and 6, and for $t > b$ by Eqs. 7, 8, and 9 are:

$$\dots - \operatorname{erfc}\left(\frac{t-b}{\sqrt{b}}\right)$$

$$\dots \left[\operatorname{erfc}\left(\frac{t-b}{\sqrt{b}}\right) - \operatorname{erfc}\left(\frac{t}{\sqrt{b}}\right) \right]$$

$$\dots \left[\operatorname{erfc}\left(\frac{t-b}{\sqrt{b}}\right) - \operatorname{erfc}\left(\frac{t}{\sqrt{b}}\right) \right]$$

$$\dots \left(\frac{t-b}{\sqrt{b}} - \frac{t}{\sqrt{b}} \right)$$

... the method of ...
 ... values of ...

by developing the solutions corresponding to Eqs. 4 and 6. It should also be noted here that Eqs. 1-3 and the solutions Eq. 4-9 are similar though not identical to those considered by Neretnieks (3) in an earlier paper addressing the potential effects of radionuclide diffusion into the bulk rock boundaries of joints containing aqueous solutions.

For an incompressible fluid in laminar, one-dimensional flow between flat, parallel plates, the average fluid velocity v appearing in the above equations is given, in consistent metric units by, (4)

$$v = \frac{1}{12\eta} \left(\frac{\Delta P}{L} \right) H^2$$

where

H = plate spacing

$\Delta P/L$ = hydraulic gradient

η = viscosity of the flowing fluid.

Provided that the assumptions made in writing Eqs. 1-3 are applicable, then for a step change in $C(C_0, t)$, mass and momentum transfer in the idealized joint are described by Eqs. 4-6 and by Eq. 10, and for a square-wave by Eqs. 7-9. For the first three assumptions made in writing Eqs. 1-3, criteria have been developed which quantitatively determine the applicability of Eqs. 4-9 in terms of the independent variables and parameters appearing in the equations. The criteria developed are restricted to the case in which t is much greater than z^2/v . However, as later shown, the results

of primary interest in these analyses are generally those
for which w is greater than z . For the flowing fluid
the criterion for the radionuclide flux due to
diffusion in the z -direction to be much greater than the flux
in the x -direction (Appendix A) is

$$z \gg w$$

and the criterion for the concentration gradient in
the x -direction (Appendix B) is

$$z \gg w$$

and the criterion for the radionuclide
flux in the x -direction to be large relative
to the z -direction (Appendix C) is

$$z \gg w$$

The descriptions made in writing Eqs. 1-3,
Eqs. 11-13 are not available.
Fick's law is generally considered
in terms of nonelectrolytes.
In aqueous solutions in which diffusion
occurs primarily between the individual ions
present at a relatively lower concentration
the use of Fick's law, rather than

...diffusion coefficient, D , is a function of the temperature, T , especially if the latter is not a very good parameter with regard to the full system. The assumption that the parabolic profile corresponds to the "average velocity" is a matter of convenience. It is a system of equations which are easily solved for the center velocity in the center of the tube. The errors introduced by this assumption are not relevant for the application.

DESIGN ANALYSIS

1. Objective, Important

The following experiment is a design:

1. The experiment employs the apparatus shown in Fig. 1. The diagram shows in Fig. 1:
2. The apparatus for injecting and for collecting the particles are applied to the system. The particles are injected into the system in a constant velocity. The particles are collected in a detector system, which is a function of the radius of the tube. The particles are collected in a detector system, which is a function of the radius of the tube.
3. The apparatus for injection and collection of the particles is a function of the radius of the tube. The particles are collected in a detector system, which is a function of the radius of the tube.

(3) then use Eqs. 4-13 to define regions of values for those key parameters which would provide optimum operating conditions and would be consistent with limitations imposed by the experimental apparatus and site; and

(4) evaluate the effects which perturbations in the parameters could have on experimental results.

Separate analyses for breakthrough curves and for activity profiles in the rock were conducted and are presented below. There was a brief discussion of the primary parameters which appear in Eqs. 4-13.

Parameters

The primary parameters appearing in Eqs. 4-13 are D , τ , F_0 , H , F_D , ρ , and μ . The parameters D , H , F_D , ρ , and μ are determined by the choice of radionuclide and by the rock formation and the experimental site. However, the velocity v and, therefore, the hydraulic gradient ∇P could be adjusted to produce the desired experimental results, given values for the other parameters.

In general, the ranges of values for D , τ , and μ are expected to be small. For example, the range of values of the diffusion coefficients at infinite dilution, (6) for many of the ionic species which could be involved in a field experiment is on the order of 0.5 to 2.0×10^{-5} or $^2/\text{sec}$ and should be a reasonable estimate of the range of values for the diffusion coefficient D . The tortuosity factor τ would be 1.0 for straight pores and larger for more tortuous paths; for instance,

The values of ϵ have been reported for various
 materials. The dielectric constant of the wall is
 assumed to be unity. The values of ϵ appear to have values on the
 order of 1.1 and 1.2 to 1.3 or ϵ^2 , respectively. It
 is assumed that the effective permeability is approximately
 unity. The values of ϵ of the wall. The apparent permeability
 is assumed to be between 20 and 30. The values of ϵ
 are assumed to be between 1.0 and 1.1. The values of the
 permeability of the wall are assumed to be between 1.0 and 1.1.
 The values of the permeability of the wall are assumed to be
 between 1.0 and 1.1. The values of the permeability of the wall
 are assumed to be between 1.0 and 1.1. The values of the permeability
 of the wall are assumed to be between 1.0 and 1.1.

Table 1

Calculated for $\epsilon = 1.1$ and $\epsilon = 1.2$

ϵ	ϵ^2	ϵ^3	ϵ^4	ϵ^5
1.1	1.21	1.331	1.4641	1.61051
1.2	1.44	1.728	2.0736	2.48832

The values of ϵ are assumed to be between 1.0 and 1.1. The values of the permeability of the wall are assumed to be between 1.0 and 1.1. The values of the permeability of the wall are assumed to be between 1.0 and 1.1.

value of H which might be encountered could be orders of magnitude larger, although it currently appears that at the experimental locations in G-Tunnel the plate spacing and initial pattern planes will be much less than one millimeter.

The range of values for the sorption equilibrium distribution coefficient K_D , is also expected to be large. Experimental data (1) show that for nuclides such as ^{22}Na , ^{137}Cs , ^{90}Sr , and ^{135}Xe , values for K_D can range from near zero to 10^4 or more greater. Furthermore, since the ranges of values for the plate spacing and distribution coefficient are large, it appears reasonable to expect that the average fluid velocity v required to obtain desired experimental results could also have a range of several orders of magnitude. However, for a given value of H , the actual range of velocities which can be obtained is limited by the range of hydraulic gradients $\Delta P/L$ which are experimentally feasible, and it currently appears that the range of values for such gradients is between 3.4×10^{-4} and 1.4×10^{-2} MPa/m (or 0.05 and 50 psi/m). Because of such relatively large ranges of values, the parameters H , K_D , and $\Delta P/L$ were considered to be the key parameters with regard to experimental design, and the following ranges were used in the analyses.

experimental site and to minimize departures from realistic hydrogeologic conditions. Breakthrough curves for a step input are considered first, and then the square-wave is considered as an attenuated step input.

Step Input. For a step input the slope of the breakthrough curve at its midpoint, $C(L,t)/C_0 = 0.5$, can be used for estimating mass transfer coefficients (9). For such an input, it then appeared that a reasonable value to choose for $C(L,t_f)/C_0$ would be somewhat greater than 0.5, say on the order of 0.7. If the hypothetical experiment under consideration involves a step change in $C(0,t)$ and if $C(L,t_f)/C_0$ given by Eq. 4 is to be about 0.7, then the corresponding value of v is about 0.27. Using the definition of v , the following expression is then obtained for the average velocity v required to give a value of $C(L,t_f)/C_0$ equal to 0.7

$$v = \frac{L}{2t_f} \left[1 - \left(1 - \frac{4t_f \bar{v}^2 D_e}{(0.27)^2 H^2} \right)^{1/2} \right] \quad (14)$$

The hydraulic gradient $\Delta P/L$ required to produce the velocity v for a particular plate spacing H is determined from Eq. 10 and must be within the range of feasible experimental values, 0.00034 to 0.34 MPa τ . Therefore, the optimum operating conditions for the experiment are determined by Eqs. 13 and 14 subject to the constraint that $0.00034 \leq \Delta P/L \leq 0.34$ MPa τ . The various combinations of values for v , H , \bar{v} , and $\Delta P/L$ which will provide these optimum operating conditions are

arranged graphically on Fig. 2, where v from Eqs. 10 and 14 is shown as a function of H for several values of the parameters μ , ρ , τ , and σ , respectively, and the previously selected values for β , L , t_p , γ , and c have been employed. The dashed line in Fig. 2 represents the criterion for the concentration gradient in the x-direction in the fluid to be small (Eq. 12). For values of v and H below the dashed line, the concentration gradient in the x-direction in the flowing fluid is small, and for values above that line, the gradient becomes large as the distance from the line increases.

As shown in Fig. 2, the combinations of parameter values which would provide optimum operating conditions are bounded by the lines for $\beta = 0.93334$, $\beta = 2.34$, $K_D = 0$, $K_D = \text{some maximum value such as } 10^4$, and by the line representing Eq. 12. More specifically, it can be seen that at small plate spacings (on the order of 10^{-3} cm) the acquisition of useful concentration curves will be limited by the maximum feasible hydraulic gradient of about 1.34 KPa/m , and at larger plate spacings, the constraints implied by the assumption that the concentration gradient in the x-direction in the flowing fluid is small (Eq. 12) and the maximum hydraulic gradient of about 1.34 KPa/m .

It is noted that, if the experiment were to involve an aqueous solution containing a plate spacing H of 10^{-3} cm, Fig. 2 indicates that the number of possible combinations of values for β , K_D , and μ is very small. The velocity, v would have to be on the order of 1.5×10^4 to 2.5×10^4 cm/day;

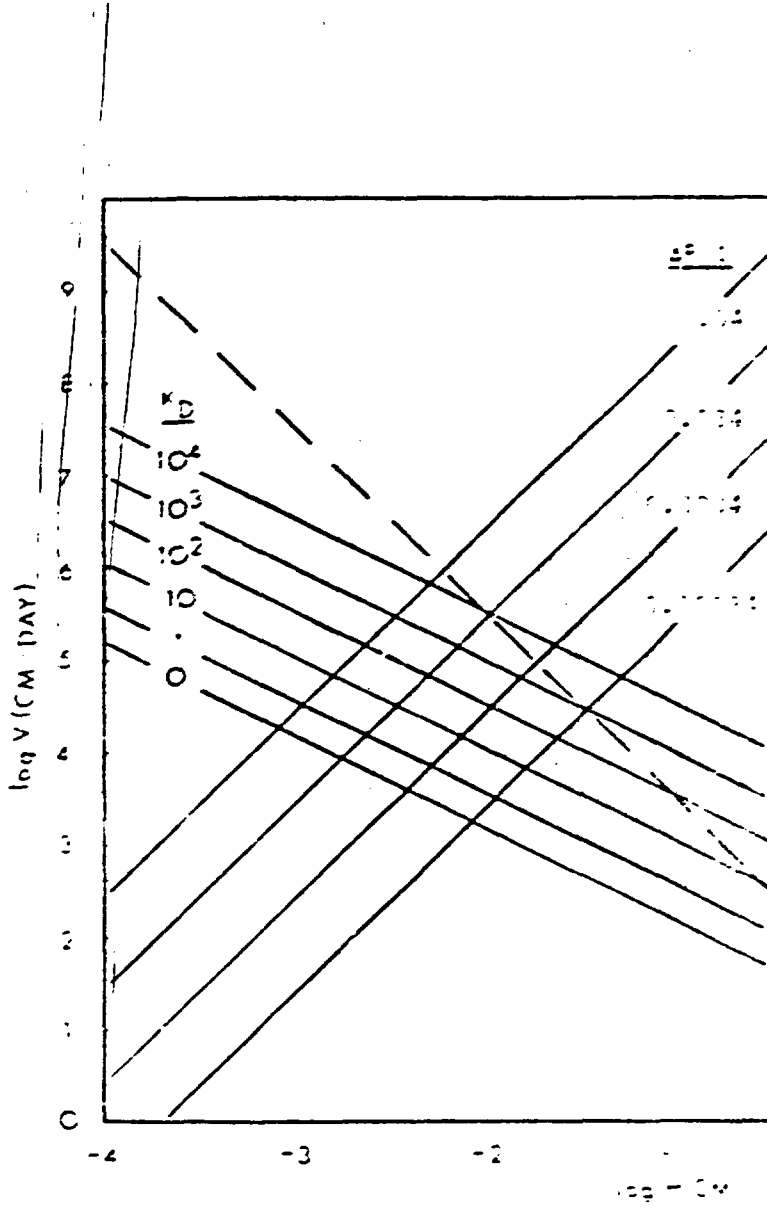
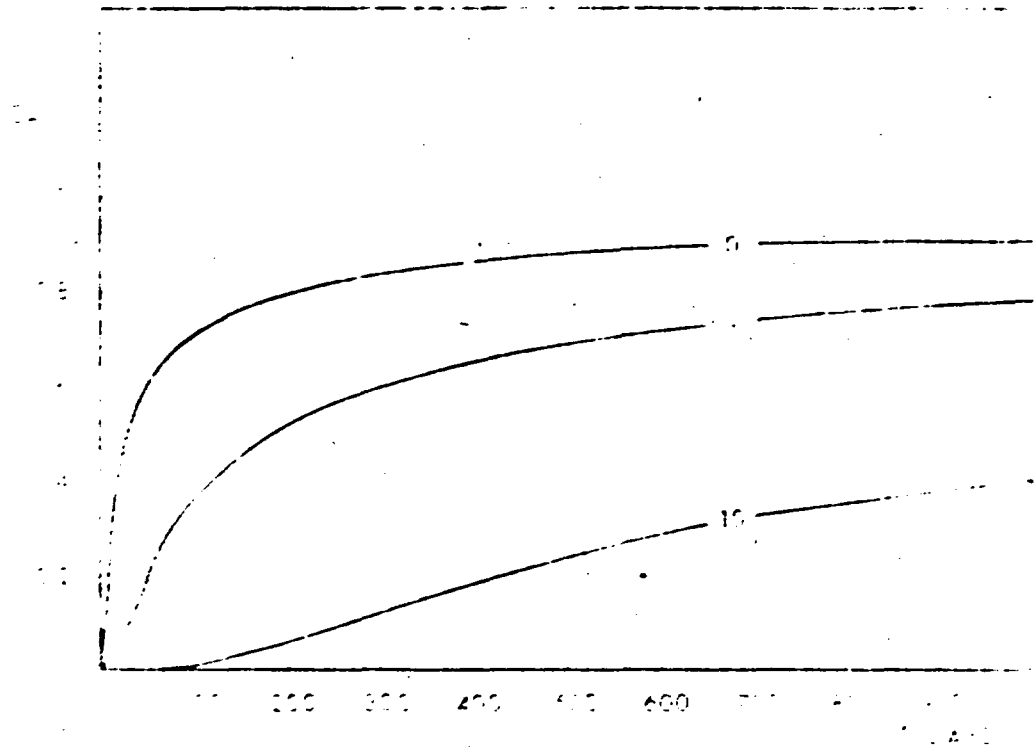


Figure 2. Water velocities produced during the flow of water through curves of Q in rivers; Q is in m^3/s .



Approximate values for the curves at various x-axis points:

X-axis	Curve 5	Curve 10	Curve 15
100	35	15	5
200	55	25	10
300	65	35	15
400	70	45	20
500	75	55	25
600	78	60	30
700	80	65	35
800	81	68	38
900	82	70	40

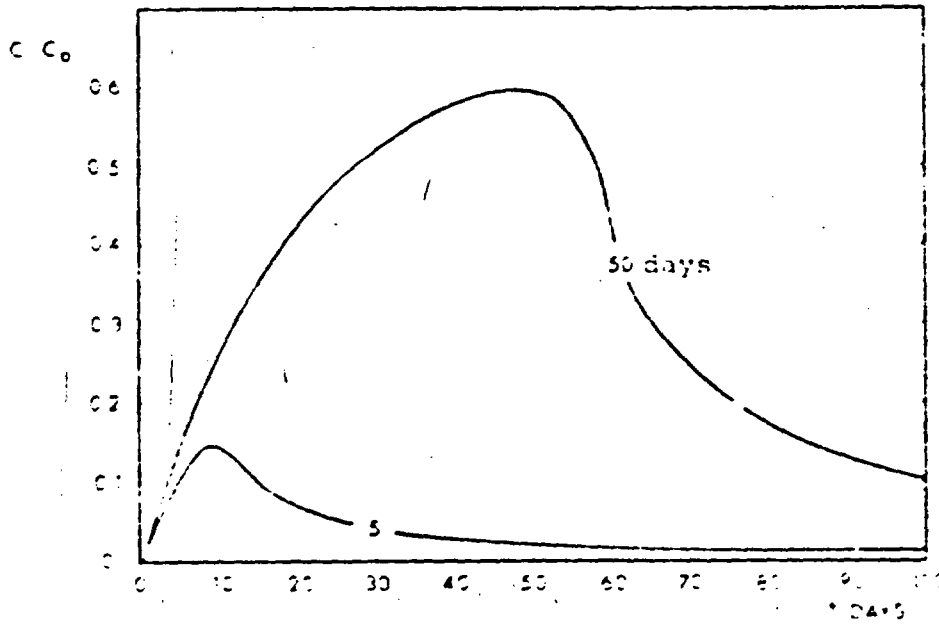


Figure 4. The influence of injection duration, t (days) on breakthrough for a square-wave input.

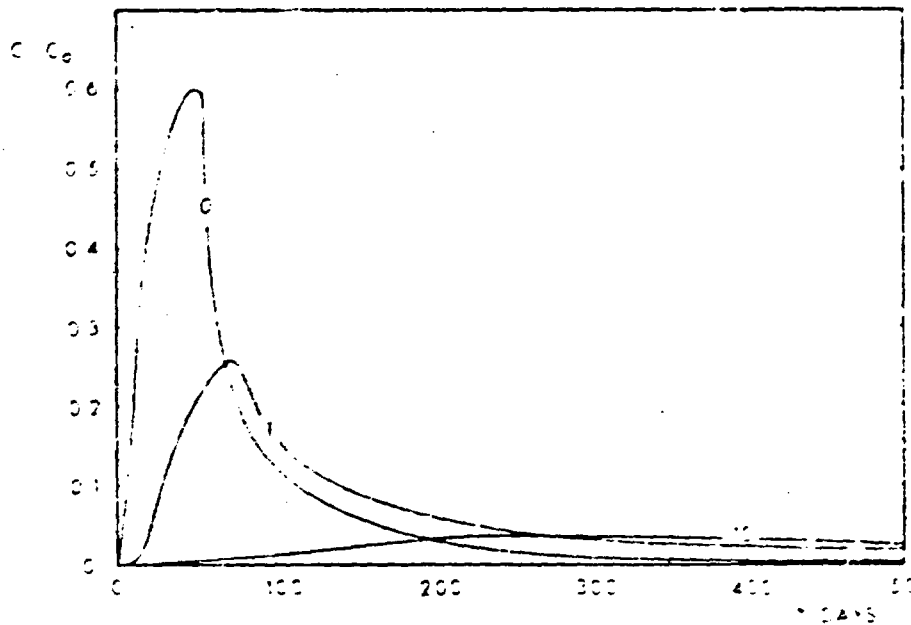


Figure 5. The dependence of breakthrough curves on K_D (ml/g) for a square-wave input.

the distribution coefficient K_D less than 1, and the hydraulic gradient H/L would have to be nearly 0.34 MPa/m. These results are further illustrated in Fig. 3 where breakthrough curves for a fluid velocity of 1.5×10^{-3} cm/day are shown for values of K_D of 0, 1, and 10 ml/gm. As can be seen from Fig. 3, for $t_p = 100$ days the curve for a value of K_D of 0 is the only one for which C/C_0 reaches 0.7, and for values of K_D on the order of 10 or greater, the breakthrough curve would essentially be nonexistent.

Square-Wave Input. For given values of H and K_D , it can be shown from Eqs. 4 and 7 and appropriate values of the complementary error function that if the optimum velocity and hydraulic gradient given by Fig. 2 are also used for a square-wave input of duration b , which is less than t_p , the resulting breakthrough curve will have a maximum value which will be less than 0.7 and which will appear at some time less than t_p . The magnitude and position of that maximum will depend on the duration of the input. For example, on Fig. 4 breakthrough curves for values of H , v , and K_D of 10^{-3} cm, 1.5×10^{-3} cm/day, and 1, respectively, are given for values of b of 5 and 50 days. It can be seen that as b decreases, the maximum value of C/C_0 decreases and shifts to smaller values of t . Also for $t < b$, the magnitude of the breakthrough curve also decreases with b and the curve becomes flatter. Therefore, the usefulness of the breakthrough curve for a given value of b will depend on the magnitude and position of the maximum value of C/C_0 and the duration of the input. Many experimental breakthrough curves

If for a given value of h , the magnitudes of the parameters and the uncertainties are not sufficiently different to permit a reasonable evaluation of proposed models, then the maximum value of C/C_0 could be increased by using a larger fluid velocity; however, as stated previously, it is recommended that minimum fluid velocities should be used. Therefore, the values of H and K_D , the optimum fluid velocity and half-saturation gradient to be used with a square-wave input can also be estimated from Fig. 2. It is then necessary to determine the input durations which will produce useful breakthrough curves for a given nuclide to be used in the experiment. For example, in Fig. 5, which is the square-wave analog to Fig. 3, breakthrough curves for values of H , v , and h of 10^{-3} cm, 1.5×10^4 cm/day, and 50 days, respectively, are shown for values of K_D of 0, 1, and 10 ml/cm. As would be predicted from Fig. 2, a value of K_D of 0 is the only one for which the shape of the breakthrough curve would be obtained by the conclusion of the experiment, and for values of K_D of 1 or 10 or greater, the breakthrough curve would essentially be nonexistent for a value of t_p equal to 100 days. For breakthrough curves corresponding to a value of K_D of 1, it appears that an input duration on the order of 100 days would provide very useful data for purposes of model evaluation. However, the usefulness of breakthrough curves for small input durations would be more dependent on the specific nuclide used.

Then using an approach similar to that taken with Breakdown curves, the following expression is obtained for the velocity v required to give a value of $g(0,1,t_p) = g_0 = 0.11$

$$v = \frac{1}{t_p} \left[1 - \left(1 - \frac{4t_p^2 H^2 D_c}{1.82)^2 H^2} \right)^{1/2} \right]$$

Again, the hydraulic gradient (P/L) required to provide the velocity v for a particular plate spacing H is determined from Eq. 11 and must be within the range of feasible experimental values. Therefore, in the case of activity profiles in the hole pack, the optimum operating conditions for the experiment are determined by Eqs. 10 and 15 subject to the constraint $0.004 < P/L < 0.14$ MPa m. The various combinations of values for $H, v, \mu,$ and P/L which will provide these optimum operating conditions are summarized graphically on Fig. 6 where the relationship between v and H is shown as a function of H for several values of the parameters P/L and K_D , respectively, and the previously selected values for $D, L, t_p, \mu, \rho,$ and γ have been used. The dashed line shown on Fig. 6 again represents the constraint given by Eq. 12. For values of v and H below the line, the concentration gradient in the x-direction in the channel flow is small, and for values above the line, the concentration gradient is larger as the distance from the line increases. As shown on Fig. 6, the combinations of parameter values which will provide optimum operating conditions are achieved for values for P/L = 0.0034, P/L = 0.04, $K_D = 1$, and

such as 10^4 . More specifically, at 10^4

the order of 10^4 in the acquisition

in the bulk rock will be limited

hydraulic gradient of about 0.04 m/m,

by the hydraulic gradient

as opposed to Fig. 2 for

the criterion given by Eq. 12 is not a

of parameter values

experimental results. Furthermore,

it can be seen that if the activity

rather than breakthrough curves,

then relative

given the same values for

therefore, it appears that the best

on the post-experiment

in the bulk rock.

if the experiment were to involve an idealized

of 10^{-3} m and a tail water column

of 10 m/m, the average flow velocity

the desired profile for g is 1.5×10^4 m/day,

would be about

it can be seen from Fig. 2 that for

breakthrough curves would

than

hydraulic

m/m.

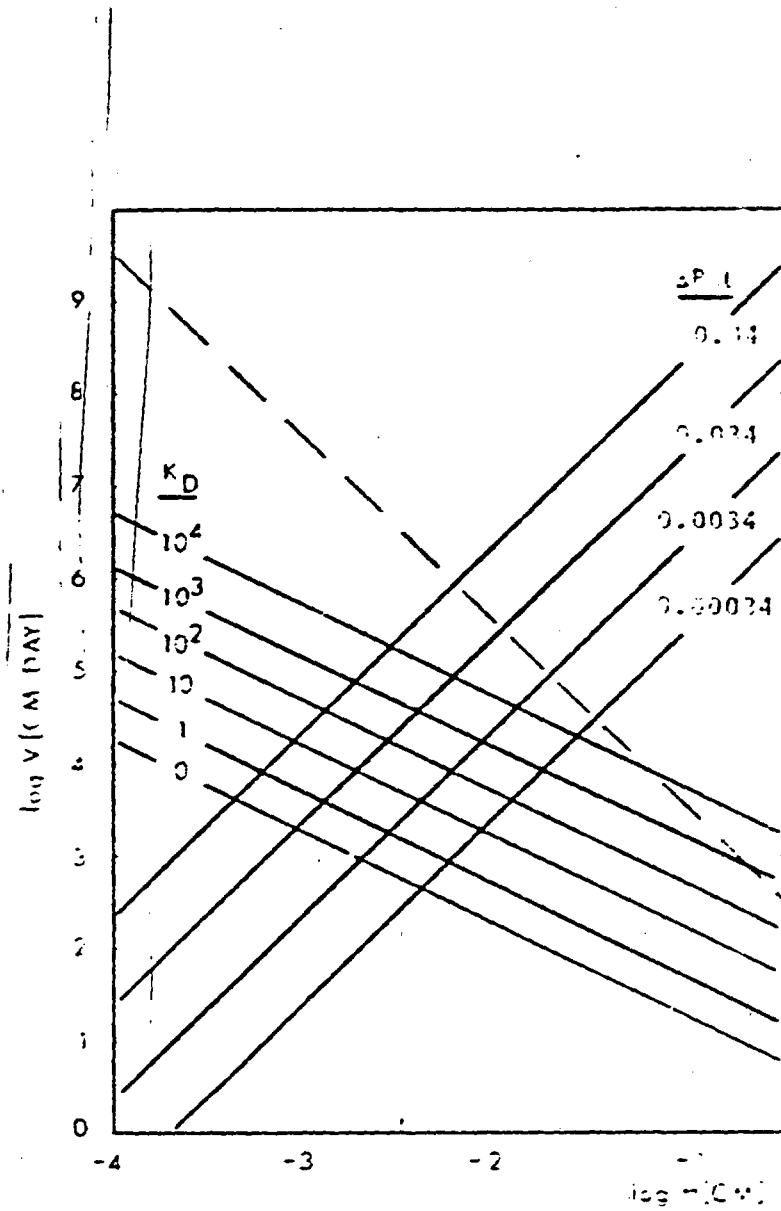
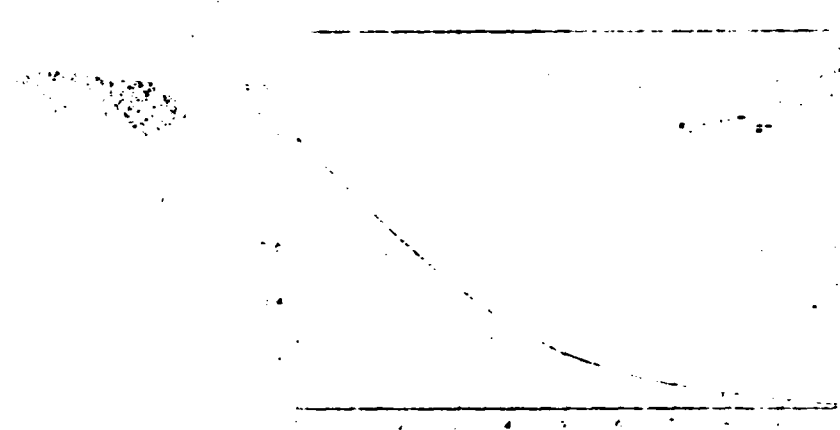
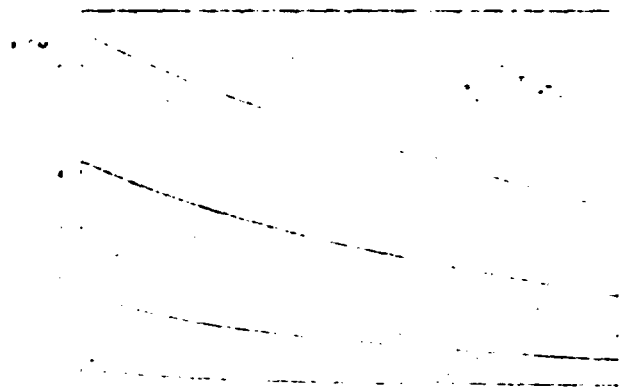


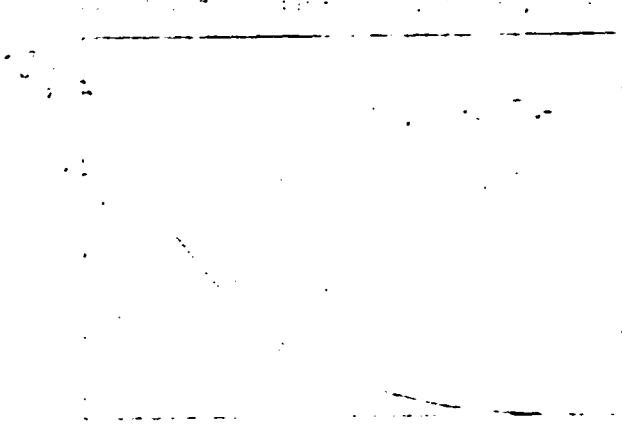
Figure 6. Water velocities producing optimum activity profiles in the bulk rock. (K_D in cm^2/day ; $\Delta P/L$ in MPa/cm).



Graph 1: $y = \frac{1}{x+1}$



Graph 2: $y = \frac{1}{x+2}$



Graph 3: $y = \frac{1}{x+5}$

The desired profile $q(0,z,t_p)/q_0$ is shown on Fig. 7, and the corresponding isoconcentration contours for the bulk rock are shown on Fig. 8 where the distance x at which values of $q(x,z,t_p)/q(0,z,t_p)$ of 0.01, 0.10, 0.50, and 0.90 occur are shown as a function of position z along the idealized joint. Since the distance x corresponding to a given value of $q(x,z,t_p)/q(0,z,t_p)$ decreases with increasing z , the profile $q(x,z,t_p)/q_0$ is somewhat steeper than $q(0,z,t_p)/q_0$ and is shown in Fig. 9.

In order to compare the results of an experiment which involves a particular combination of parameter values obtained in Fig. 10 with the results of similar experiments involving other combinations in those parameter values, the plate spacing of 1.5 cm, distribution coefficient of 10 ml/gm, and average flow velocity of 1.5×10^{-7} cm/day were selected as a base case. The profiles resulting from changing one of those three variables while holding the other two constant were then obtained and compared with the profile for the base case. In Fig. 10 values of $q(0,z,t)/q_0$ are shown as a function of z for several values of K_D ; in Fig. 11 for several values of v , and in Fig. 12 for several values of H . As shown by the three figures, variations in the magnitude of the velocity v and plate spacing H can cause much greater deviations from the desired profile than can similar variations in the magnitude of the distribution coefficient K_D . For some additional comparisons, the profile $Q(z,t_p)/q_0$ and the isoconcentration contour for $q(x,z,t_p)/q(0,z,t_p) = 0.1$ are shown for several

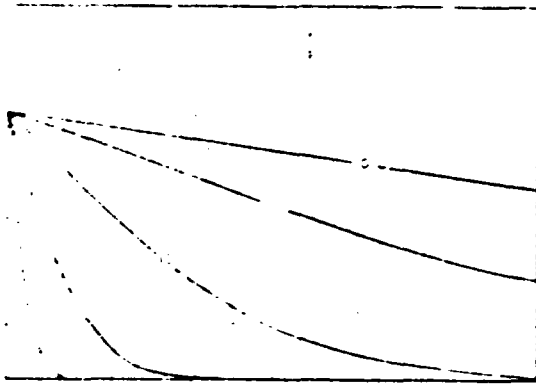


Figure 1: Surface activity profile of C_{12}E_8 at $\text{C}_0 = 1.5 \times 10^{-3}$ mol/l and $H = 1.5$ cm.

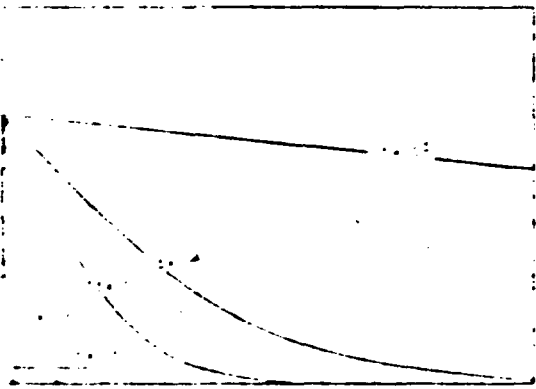


Figure 2: Surface activity profile of C_{12}E_8 at $\text{C}_0 = 1.5 \times 10^{-3}$ mol/l and $H = 1.5$ cm.

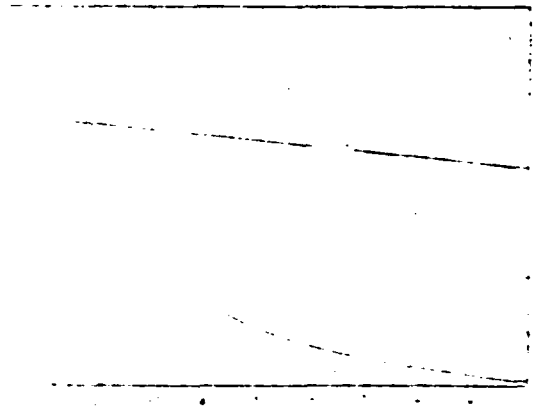


Figure 3: Surface activity profile of C_{12}E_8 at $\text{C}_0 = 1.5 \times 10^{-3}$ mol/l and $H = 1.5$ cm.

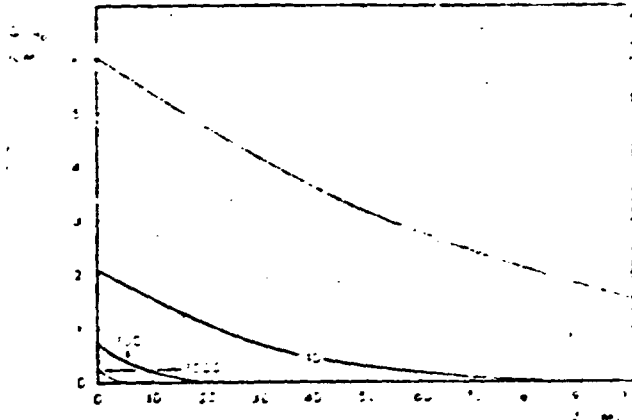


Figure 13(a). The dependence of total solid-phase retention C_0 on F_D (ml/cm) for $v = 1.5 \times 10^4$ cm/day and $H = 10^{-3}$ cm.

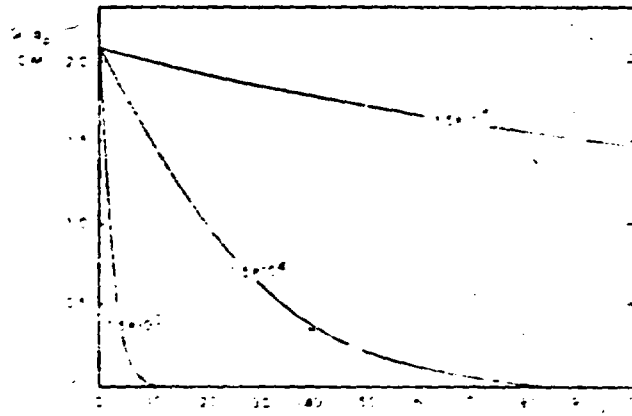


Figure 13(b). The dependence on v (cm/day) for $F_D = 10$ ml/cm and $H = 10^{-3}$ cm.

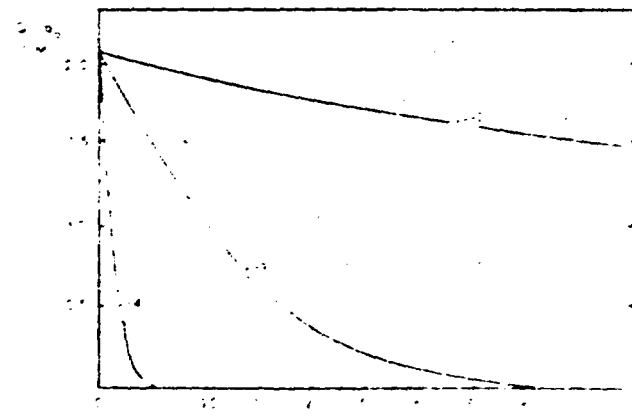


Figure 13(c). The dependence on H (cm) for $v = 1.5 \times 10^4$ cm/day and $F_D = 10$ ml/cm.

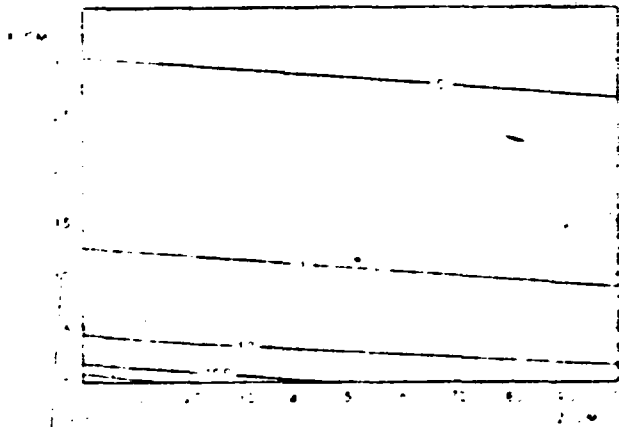
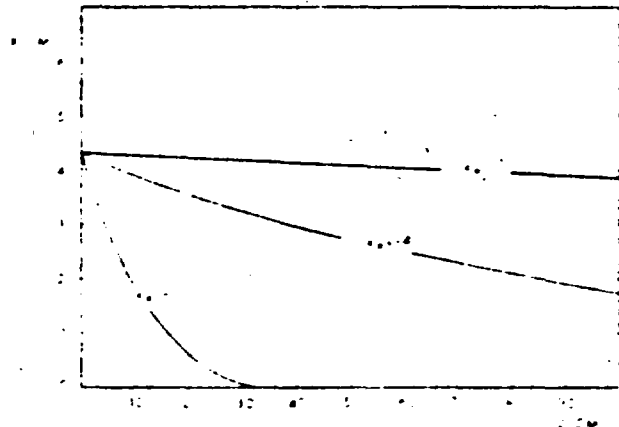
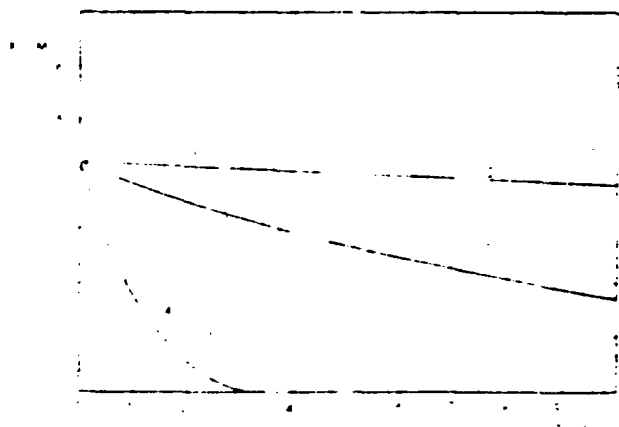


Figure 4(a). The dependence of the 10% isocentration on distance x (cm) for $v = 1.5 \times 10^4 \text{ cm/day}$ and $H = 10^{-2} \text{ cm}$.



(b) The dependence on v (cm/day) for $E_0 = 10 \text{ cm}$ and $H = 10^{-2} \text{ cm}$.



The dependence on v (cm/day) for $E_0 = 10 \text{ cm}$ and $H = 10^{-2} \text{ cm}$.

values of K_2 , v , and H on Figs. 13 and 14, respectively.

In particular, from Fig. 14 it appears that in addition to the independence of the activity profiles, the magnitude of K_2 will also provide such valuable data for purposes of model evaluation when the value of K_2 is on the order of 0 to 1000000.

Since the range of values estimated for the parameters K_1 , K_2 , and v were small, perturbations which are introduced in these parameter values should cause relatively small deviations from the desired profile. As an example, in the case of values of H , K_2 , and v , Fig. 15 shows a plot of z for several values of the wind fraction f . Finally, Fig. 16 illustrates the effects of deviations in the duration b of the experiment. In particular, the profiles for 100 days is compared with those for durations of 20 and 30 days. Also, the profiles corresponding to the base case values of H and K_2 at a velocity v of 1.5×10^5 or day are shown for values of b of 10^2 and 10^4 days.

4.1.2.2. Input Duration. For the base case values of H , K_2 , and v and for input durations b of 20, 50, and 30 days, the profiles of z , z_1/q_0 , and z_2/q_0 were calculated and are compared with those for a step input on Figs. 17 and 18, respectively. As illustrated by the figures, the profiles for impulsive input have a maximum between $z = 0$ and $z = 1$ and $z = 1$. Furthermore, the profiles become flatter as the input duration b decreases, and the profiles' usefulness for validation purposes will depend on the relative magnitudes of the input values of b , q_1 , and z_1/q_0 and the uncertainties

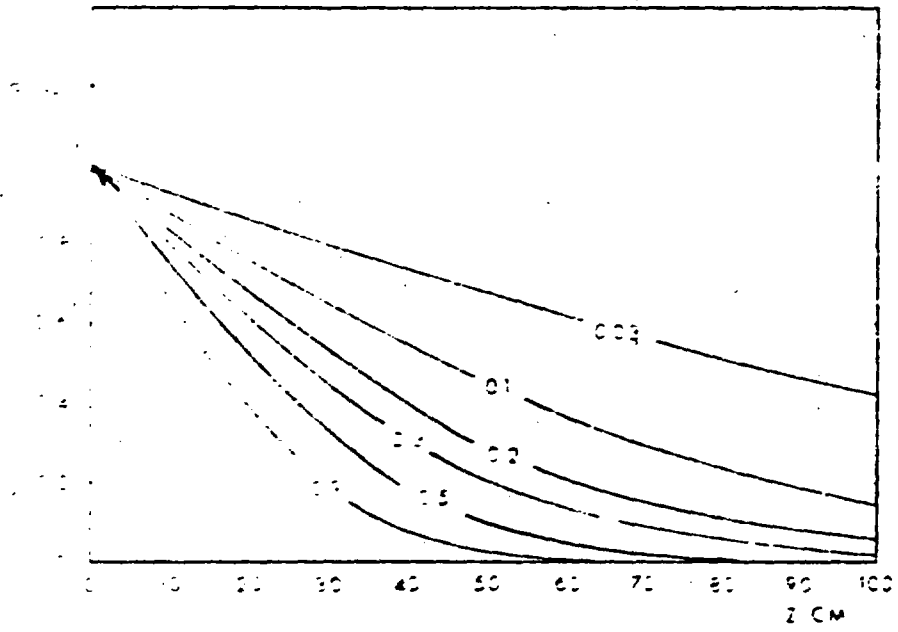


Figure 10. The dependence of surface activity profile on the fraction, f .

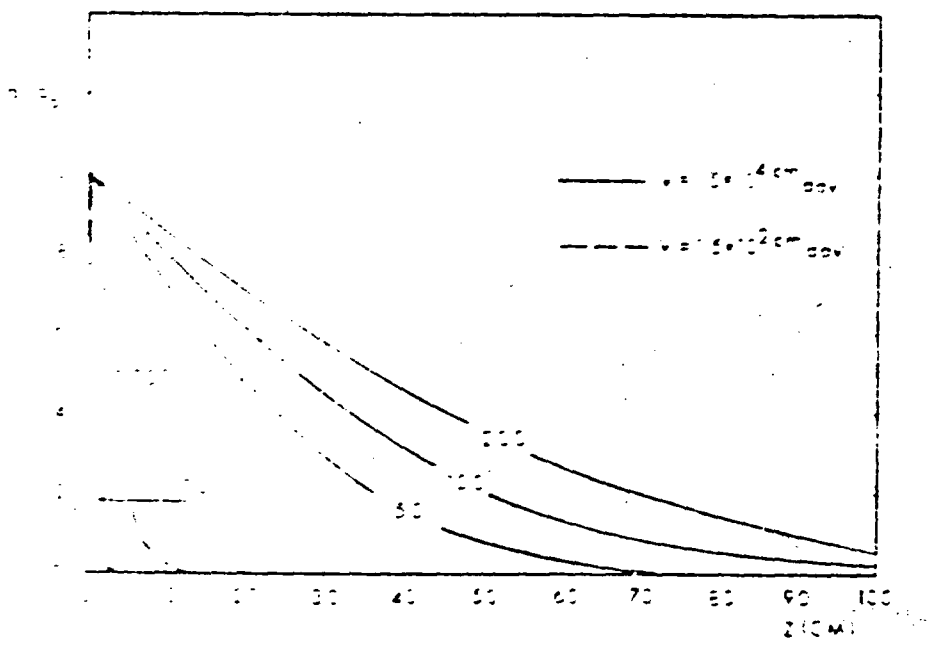


Figure 11. Dependence of surface activity profiles on experiment duration, t_e , days.

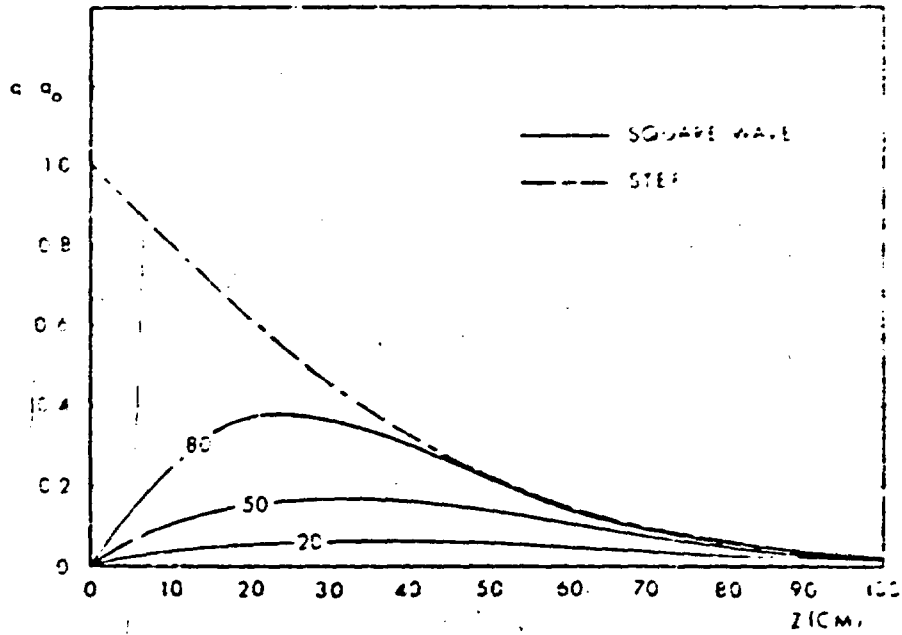


Figure 17. The dependence of surface activity profile on tracer input duration, b (days).

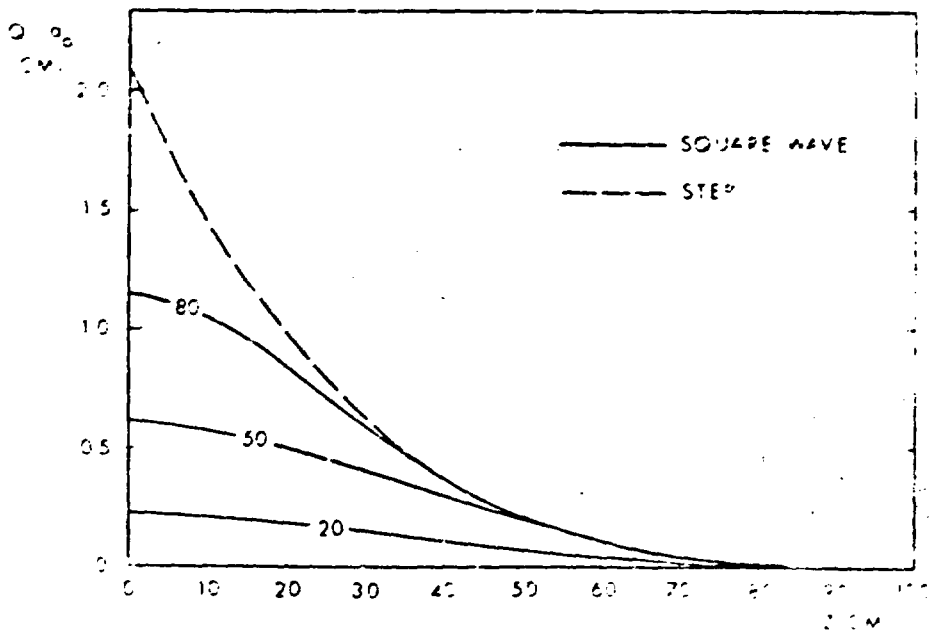


Figure 18. The dependence of total solid-phase activity profile on tracer input duration, b (days).

in obtaining experimental profiles in the bulk region. In fact, when the value of b , the magnitudes of the maxima and the uncertainties are not sufficiently different to permit a valid evaluation of proposed models, then the accuracy of a and b could be increased by using a higher fluid velocity; however, as stated before, it is felt that higher velocities should be used. Therefore, given values of a and b , the optimal fluid velocity and a travel distance with a square-wave input can also be estimated from the model, but it is then again necessary to determine the input profile which will produce useful activity profiles for the reactor.

DISCUSSION

Results of the Synthesis Experiment

The principal results of the system analyses for the synthesis experiment are summarized as follows:

1. The measured rates in the bulk tank should be directly related to the source experimental data.
2. The data can be determined by just one experiment.
3. The transient response can be determined with a single experiment.
4. The activity profiles in both the reactor and the bulk tank can be determined by just one experiment.
5. The activity profiles in both the reactor and the bulk tank can be determined by just one experiment.

- (2) The use of breakthrough curves could have advantages in specific applications. For example, the analysis of breakthrough curves for nonsorbing or slightly sorbing solutes could be used for the in situ characterization of the residence-time-distribution of the fluid flowing in an actual point. Also the breakthrough curve essentially provides a real-time record for the experiment.
- (3) A step change in concentration at $t = 0$ should generally provide as good or better data for purposes of model evaluation than will a square-wave. However, use of a square-wave input may have advantages for specific purposes, such as examining reversibility of sorption phenomena.
- (4) The primary parameters controlling radionuclide transport are the plate spacing H , fluid velocity v , and distribution coefficient K_D . The required hydraulic gradient $\Delta P/L$ is then determined from v and H .
- (5) If the data from the experiment are to provide for accurate evaluation of proposed models, then given values of H and K_D , the optimum values of v and $\Delta P/L$ can be obtained from Figs. 3 and 6 for breakthrough curves and activity profiles in the bulk rock, respectively.

... the
... ..

... desired profiles in the bulk rock
... more sensitive to plate spacing H and
... to a specific distribution coefficient

... velocity to be used in an experiment will
... the necessity to keep the velocity as
... in order to minimize possible
... the experiment site and to minimize
... realistic by the above conditions.

... velocity for a specific value of n is
... the
... of that line is unity, the minimum
... ..

... ..
... the minimum volumetric flow rate,
... of the idealized system, is the
... ..
... ..

... ..
... ..
... ..
... ..
... ..

Implications for an Actual Experiment

The transport of fluid machines in a real point is naturally predicted from that calculated for the hypothetical case. However, if the physical machine characteristics for the idealized case are also the characteristics for the real point, then the hypothetical experiment would provide a more accurate prediction of the actual experiment.

The breakthrough curves and bulk-averaged characteristics obtained from an actual experiment probably will differ relative to those calculated for the hypothetical case. These differences would result from the actual characteristics of a real point, such as a number of physical and varying physical and chemical parameters. The relative changes in the behavior of a real experiment will result from perturbations in parameters such as μ , σ , and τ . Changes in the behavior of the hypothetical case are shown as those shown on Figs. 2, 3, 4, 5, and 6.

The relative relationships between μ , σ , τ , and ρ shown by Figs. 2 and 6 should be similar for a real point. However, due to the nature of a real point the value of ρ will probably be larger than for the hypothetical case, and Figs. 3 and 6 can present a more accurate prediction of the actual experiment. The relative relationships between μ , σ , τ , and ρ shown by Figs. 4 and 5 should be similar for a real point. However, due to the nature of a real point the value of ρ will probably be larger than for the hypothetical case, and Figs. 4 and 5 can present a more accurate prediction of the actual experiment. The relative relationships between μ , σ , τ , and ρ shown by Figs. 5 and 6 should be similar for a real point. However, due to the nature of a real point the value of ρ will probably be larger than for the hypothetical case, and Figs. 5 and 6 can present a more accurate prediction of the actual experiment.

in the z-direction in the flowing fluid, small concentration gradients in the x-direction in the flowing fluid, and negligible diffusion in the z-direction in the bulk rock. Furthermore, the use of Fick's law in similar situations is reasonably well supported by the literature, and the errors incurred by replacing the parabolic profile with an average velocity can be shown to be small. The parabolic profile could be used in a more exact model. The elements in the definition of the idealized point are essentially be divided into two categories: (1) those which are related to the physical and chemical phenomena determining the transfer (and which may, therefore, depend on the size, shape, and radionuclide and concentration used), and (2) those which are related to the uniform cross section of the point and to the uniform and continuous physicochemical properties of the bulk rock.

Since the applicability of the assumptions made in Eqs. 1-3 is reasonably well defined, the experimental and theoretical investigations should be designed and conducted to determine if the phenomena represented in Eqs. 1-3 are in fact which dominate radionuclide transport in an actual point. If terms for additional processes should be included in the transport model. Additionally, the investigations should check for nonuniformities in the cross sections for actual points and the properties of the rock, and appropriate methods should be developed for incorporating the effects of these nonuniformities into the model.

CONCLUSIONS AND RECOMMENDATIONS

The results of the above-mentioned initial evidence
from the field experiments. An experimental
program should be devised to identify any
relationships between the transport and
retention of particles in the sediment, physical, and
chemical properties of the water. It is anticipated that initial
studies should involve especially simple models which
describe the transport of particles in the field case.
The analysis indicates that the particle
size distribution has a relatively larger impact
on the rate than the distribution coefficient K_d .
Further studies should be given to the investigation
of these factors.

REFERENCES

1. F. L. Erickson, unpublished work.
2. H. S. Carslaw and J. C. Jaeger, Conduction of Heat in Solids, 2nd ed., Oxford University Press, p. 396 (1973).
3. I. Meretnieks, "Diffusion in the Rock Matrix: A Factor in Radionuclide Retardation?" Journal of Environmental Research, V. 85, No. B8, pp. 4379-4397 (1973).
4. I. H. Shames, Mechanics of Fluids, McGraw-Hill, N.Y., pp. 288-290 (1962).
5. R. B. Bird, W. E. Stewart, and E. N. Lightfoot, Transport Phenomena, John Wiley & Sons, New York, p. 557 (1960).
6. J. S. Newman, Electrochemical Systems, Prentice-Hall, Englewood Cliffs, N.J., pp. 217-238 (1973).
7. Y. Li and S. Gregory, "Diffusion of Ions in Sediments in Deep-Sea Sediments," Geochimica et Cosmochimica Acta, V. 38, pp. 703-714 (1974).
8. A. R. Lippin, unpublished work.
9. T. H. Sherwood, R. L. Pigford, and C. R. Wilke, Mass Transfer, McGraw-Hill, N.Y., pp. 565-579 (1975).

APPENDICES

1. THE EFFECT OF DIFFUSION IN THE ...

... transport of ...

... that results ...

...

...

$$K_1 \dots$$

...

or

$$\frac{2}{\pi} \frac{D}{w^2} \frac{1}{\exp(-2) \operatorname{erfc}(r)} \ll 1.$$

The maximum value of $\frac{2}{\pi} \frac{D}{w^2} \frac{1}{\exp(-2) \operatorname{erfc}(r)}$ which would be of interest probably corresponds to a value of C/C_0 of about 0.51, and is, therefore, approximately equal to 6.4. The above inequality then becomes

$$6.4 \frac{D}{w^2} \ll 1$$

and for practical purposes, the desired criterion can be stated as

$$w^2 \gg 7D \quad (t \gg z/w).$$

3. Criterion for Small Concentration Gradients in the x-direction in the Flowing Fluid.

If the concentration gradient in the x-direction in the flowing fluid is to be small, then the difference ΔC between the concentration along the middle plane between plates and the concentration at the fluid-rock interface should be small relative to the average concentration, C . If the average concentration gradient $(\partial C / \partial x)_{\text{avg}}$ in the fluid were known, the term ΔC could be obtained from

$$\Delta C = \frac{H}{2} \left(\frac{\partial C}{\partial x} \right)_{\text{avg}}$$

Since the magnitude of the concentration gradient in the flowing fluid generally increases nonlinearly as the fluid-rock interface is approached, and since the gradient along the middle plane is zero, the average gradient will be less than one-half of the concentration gradient at the fluid-rock interface. For the purposes of these calculations, the average gradient was taken as one-third of the gradient at the interface. Thus, since

$$D \frac{\partial c}{\partial x} = D_e \frac{\partial c}{\partial x}$$

at the fluid-rock interface, the criterion for small concentration gradients in the x-direction in the flowing fluid can be stated as

$$-\frac{1}{3} \frac{D_e}{D} \left(\frac{\partial c}{\partial x} \Big|_{x=0} \right) \ll 1.$$

Assuming again that the results for a step input would be typical, the concentration c is given by

$$c = c_0 \operatorname{erfc} \left(\frac{x}{2 \sqrt{D_e t}} \right)$$

where $c_0 = C_0 F$, and for $t \gg z^2 / v$, $t \gg z^2 / D_e$. Now,

$$\frac{\partial c}{\partial x} = -\frac{c_0 F \exp(-x^2 / 4 D_e t)}{\sqrt{D_e t}}$$

$$C = C_0 \operatorname{erfc}(\cdot)$$

Therefore, the preceding inequality can be written:

$$\left[\frac{1}{\operatorname{erfc}(\cdot)} \right] \frac{1}{6.4} \frac{H}{D} \frac{\sqrt{K_1 D}}{\sqrt{t}} \exp(-\cdot^2) < 1$$

Then since

$$\left(\frac{z}{H} \frac{\sqrt{K_1 D}}{\sqrt{t}} \right) \frac{H}{z} = \frac{H}{z}$$

the above inequality becomes

$$\frac{1}{6.4} \frac{H^2}{D} \frac{1}{z^2} \frac{1}{\exp(-\cdot^2) \operatorname{erfc}(\cdot)} < 1$$

$$\frac{z}{H} \geq \frac{1}{6.4} \frac{H^2}{D} \frac{1}{\exp(-\cdot^2) \operatorname{erfc}(\cdot)}$$

The maximum value of $z/\exp(-\cdot^2) \operatorname{erfc}(\cdot)$ which would be

obtained probably corresponds to a value of C/C_0 of 0.25.

It is, therefore, approximately equal to 6.4. The inequality for

z/H then becomes

$$\frac{z}{H} \geq 0.6 \frac{H^2}{D}$$

Furthermore, it appears reasonable that the ratio $\frac{J_z}{J_x}$ should be small or less. In which case, the desired criterion can be written as

$$\frac{J_z}{J_x} \ll 1 \quad (1)$$

1. Criterion for Neglecting Diffusion in the z-direction in the Bulk Phase.

If the flux due to molecular diffusion in the z-direction is small relative to the flux due to molecular diffusion in the x-direction, then

$$\frac{J_z}{J_x} \ll 1$$

Assuming again that the results for a step input would be applicable, the concentration C is given by

$$C(x,z,t) = \frac{C_0}{2\sqrt{\pi D_x t}} \exp\left(-\frac{x^2}{4D_x t}\right) \exp\left(-\frac{z^2}{4D_z t}\right)$$

where C_0 is the initial concentration.

Therefore

$$\frac{J_z}{J_x} = \frac{D_z}{D_x} \frac{z}{x}$$

$$\frac{hc}{2z} = \frac{hc}{2z} \frac{\bar{K} \sqrt{D_e}}{Hv\sqrt{t}}$$

the preceding inequality reduces to

$$\frac{Hv}{2\bar{K}D_e} \gg 1.$$

Furthermore,

$$\bar{K}D_e = zD/v^2$$

and

$$Hv \gg \frac{2zD}{2} \quad (t \gg z/v).$$

Attribution:

D. A. Math, Director
Office of Waste Isolation
U. S. Department of Energy
Room B-207
Germantown, MD 20737

D. A. Math, Acting Team Leader
Technology Team
U. S. Department of Energy
Room B-220
Germantown, MD 20737

J. C. Neff, Program Manager
National Waste Terminal
Storage Program Office
U. S. Department of Energy
305 King Avenue
Columbus, OH 43201

J. L. Ramspott
Technical Project Officer
Lawrence Livermore National
Laboratory
University of California
P. O. Box 808
Mail Stop L-204
Livermore, CA 94550

J. E. Erdal
Technical Project Officer
Lawrence Livermore National Laboratory
University of California
P. O. Box 1663
Mail Stop 514
Livermore, CA 94545

J. E. Erdal
1100 E Street
Livermore, CA 94550

J. E. Erdal
Technical Project Officer
U. S. Geological Survey
P. O. Box 25046
Mail Stop 954
Federal Center
Denver, CO 80301

W. E. Wilson
U. S. Geological Survey
P. O. Box 25046
Mail Stop 954
Denver, CO 80301

A. R. Hakl, Site Manager
Westinghouse - AESD
P. O. Box 708
Mail Stop 703
Mercury, NV 89023

K. Street, Jr.
Lawrence Livermore National
Laboratories
University of California
Mail Stop L-299
P. O. Box 808
Livermore, CA 94550

N. E. Carter
Battelle
Office of Nuclear Waste
Isolation
505 King Avenue
Columbus, OH 43201

W. A. Carbiener
Battelle
Office of NWTIS Integration
505 King Avenue
Columbus, OH 43201

C. R. Cooley, Deputy Director
Office of Waste Isolation
U. S. Department of Energy
Room B-214
Germantown, MD 20767

R. G. Goranson
U. S. Department of Energy
Richland Operations Office
P. O. Box 550
Richland, WA 99352

S. Deau
Rockwell International
Materials International Div.
Rockwell Hanford Operations
Richland, WA 99352

R. M. Nelson, Jr., Director (3)
Waste Management Project Office
U. S. Department of Energy
P. O. Box 14100
Las Vegas, NV 89114

R. E. Miller, Director
Office of Public Affairs
U. S. Department of Energy
P. O. Box 14100
Las Vegas, NV 89114

R. H. Marks
U. S. Department of Energy
CP-1, W S 210
P. O. Box 14100
Las Vegas, NV 89114

R. W. Church, Director
Health Physics Division
U. S. Department of Energy
P. O. Box 14100
Las Vegas, NV 89114

R. E. Leux (7)
U. S. Department of Energy
P. O. Box 14100
Las Vegas, NV 89114

R. J. Marola
Colines & Karver, Inc.
Post Office Box 14340
Las Vegas, NV 89114

R. Goldsmith
Battelle
Office of Nuclear Waste
Isolation
505 King Avenue
Columbus, Ohio 43201

W. Library (5)
Battelle
Office of Nuclear Waste
Isolation
505 King Avenue
Columbus, Ohio 43201

R. J. Hill
State Planning Consultant
Governor's Office
State of Nevada
Capital City
Carson City, NV 89401

N. A. Clark
Department of Energy
State of Nevada
Capital Complex
Carson City, NV 89401

J. F. Seltzer
International Atomic Energy
Agency
Division of Nuclear Power
and Reactors
Karlter Ring 11
P. O. Box 590, A-1011
Vienna, Austria

H. F. Cunningham
Reynolds Electrical & Instrument
Co., Inc.
Mail Stop 555
P. O. Box 14400
Las Vegas, NV 89114

J. A. Cross
Fenix & Scissari, Inc.
P. O. Box 15400
Las Vegas, NV 89114

A. M. Friedman
Argonne National Laboratory
9700 S. Cass Avenue
Argonne, IL 60439

Distribution:

R. C. Hoffman, LANL
G. W. Anderson, LANL

- 4537 W. W. Miller
- 4539 W. W. Lynch
- 4537 C. J. Jurek
- 4537 W. P. Hartney (4)
- 4537 J. E. Hester
- 4537 A. P. Lippin
- 4537 G. D. Tyler
- 4538 W. G. Lincoln
- 4538 A. E. Stephenson
- 4522 E. F. Wilson
- 4500 R. S. Claassen
- Adm.: 5810 P. G. Kepler
- 5820 P. E. Khan
- 5830 M. J. Davis
- 7840 L. E. Magnum
- 7840 D. W. Schaefer
- 7840 C. H. Northrup
- 7840 F. L. Erickson (4)
- 7840 E. C. Pittali
- 7840 E. C. Moran
- 7840 L. E. Beauchamp
- 8141 L. Erickson (5)
- 8151 G. L. Garner (3)
- 8153-3 J. Balin

(or DD FORM 100) (unlimited release)